

# Antennas and Reaction Centers of Photosynthetic Bacteria

Structure, Interactions, and Dynamics

Proceedings of an International Workshop  
Feldafing, Bavaria, F.R.G., March 23–25, 1985

Editor: M. E. Michel-Beyerle

With 168 Figures

Springer-Verlag  
Berlin Heidelberg New York Tokyo

## Contents

---

Part I	Antennas: Structure and Energy Transfer	
	Structure of Antenna Polypeptides. By H. Zuber .....	2
	The Crystal and Molecular Structure of C-Phycocyanin By R. Huber .....	15
	C-Phycocyanin from <i>Mastigocladus laminosus</i> . Isolation and Properties of Subunits and Small Aggregates. By W. John, R. Fischer, S. Siebzehnrübl, and H. Scheer (With 9 Figures) .....	17
	Picosecond Time-Resolved, Polarized Fluorescence Decay of Phycobilisomes and Constituent Biliproteins Isolated from <i>Mastigocladus laminosus</i> By S. Schneider, P. Geiselhart, T. Mindl, F. Dörr, W. John, R. Fischer, and H. Scheer (With 4 Figures) .....	26
	Fluorescence Behaviour of Crystallized C-Phycocyanin (Trimer) from <i>Mastigocladus laminosus</i> By S. Schneider, P. Geiselhart, C. Scharnagl, T. Schirmer, W. Bode, W. Sidler, and H. Zuber (With 4 Figures) .....	36
	Energy-Transfer Kinetics in Phycobilisomes By A.R. Holzwarth (With 2 Figures) .....	45
	Exciton State and Energy Transfer in Bacterial Membranes: The Role of Pigment-Protein Cyclic Unit Structures By R.M. Pearlstein and H. Zuber .....	53
	Carotenoid-Bacteriochlorophyll Interactions By R.J. Cogdell (With 1 Figure) .....	62
	Bacteriochlorophyll <i>a</i> - and <i>c</i> -Protein Complexes from Chlorosomes of Green Sulfur Bacteria Compared with Bacteriochlorophyll <i>c</i> Aggregates in CH <sub>2</sub> Cl <sub>2</sub> -Hexane. By J.M. Olson, P.D. Gerola, G.H. van Brakel, R.F. Meiburg, and H. Vasmel (With 8 Figures) ...	67
	Reverse-Phase High-Performance Liquid Chromatography of Antenna Pigment- and Chlorosomal Proteins of <i>Chloroflexus</i> <i>aurantiacus</i> . By R. Feick (With 2 Figures) .....	74

Fluorescence-Detected Magnetic Resonance of the Antenna Bacteriochlorophyll Triplet States of Purple Photosynthetic Bacteria. By A. Angerhofer, J.U. von Schütz, and H.C. Wolf (With 1 Figure) .....	78
High-Resolution <sup>1</sup> H NMR of Light-Harvesting Chlorophyll- Proteins. By C. Dijkema, G.F.W. Searle, and T.J. Schaafsma .....	81
Crystallization and Linear Dichroism Measurements of the B800- 850 Antenna Pigment-Protein Complex from <i>Rhodopseudomonas</i> <i>sphaeroides</i> 2.4.1 By J.P. Allen, R. Theiler, and G. Feher (With 2 Figures) .....	82
Crystallization of the B800-850-complex from <i>Rhodopseudomonas</i> <i>acidophila</i> Strain 7750 By R.J. Cogdell, K. Woolley, R.C. Mackenzie, J.G. Lindsay, H. Michel, J. Dobler, and W. Zinth (With 6 Figures) .....	85
Linear Dichroism (LD) and Absorption Spectra of Crystals of B800-850 Light-Harvesting Complexes of <i>Rhodopseudomonas</i> <i>capsulata</i> . By W. Mäntele, K. Steck, T. Wacker, W. Welte, B. Levoir, and J. Breton (With 5 Figures) .....	88

---

**Part II            Reaction Centers: Structure and Interactions**

---

The Crystal Structure of the Photosynthetic Reaction Center from <i>Rhodopseudomonas viridis</i> By J. Deisenhofer and H. Michel (With 2 Figures) .....	94
Single Crystals from Reaction Centers of <i>Rhodopseudomonas viridis</i> Studied by Polarized Light. By W. Zinth, M. Sander, J. Dobler, W. Kaiser, and H. Michel (With 3 Figures) .....	97
On the Analysis of Optical Spectra of <i>Rhodopseudomonas viridis</i> Reaction Centers By E.W. Knapp and S.F. Fischer (With 3 Figures) .....	103
Orientation of the Chromophores in the Reaction Center of <i>Rhodopseudomonas viridis</i> . Comparison of Low-Temperature Linear Dichroism Spectra with a Model Derived from X-Ray Crystallography. By J. Breton (With 4 Figures) .....	109
Calculations of Spectroscopic Properties of Bacterial Reaction Centers. By W.W. Parson, A. Scherz, and A. Warshel (With 5 Figures) .....	122
On the Temperature-Dependence of the Long Wavelength Fluorescence and Absorption of <i>Rhodopseudomonas viridis</i> Reaction Centers. By P.O.J. Scherer, S.F. Fischer, J.K.H. Hörber, M.E. Michel-Beyerle, and H. Michel (With 3 Figures) .....	131

Local Environments of Pigments in Reaction Centers of Photosynthetic Bacteria from Resonance Raman Data By M. Lutz and B. Robert (With 4 Figures) .....	138
The Spin-Polarization Pattern of the $\Delta m = 1$ Triplet EPR Spectrum of <i>Rps. viridis</i> Reaction Centers By F.G.H. van Wijk, P. Gast, and T.J. Schaafsma .....	146
Triplet State Investigation of Charge Separation and Symmetry in Single Crystals of <i>R. viridis</i> Reaction Centers By J.R. Norris, D.E. Budil, H.L. Crespi, M.K. Bowman, P. Gast, C.P. Lin, C.H. Chang, and M. Schiffer .....	147
Triplet-minus-Singlet Absorbance Difference Spectroscopy of Photosynthetic Reaction Centers by Absorbance-Detected Magnetic Resonance. By A.J. Hoff (With 11 Figures) .....	150
ENDOR Studies of the Primary Donor in Bacterial Reaction Centers. By W. Lubitz, F. Lenzian, M. Plato, K. Möbius, and E. Tränkle (With 6 Figures) .....	164
ENDOR of Semiquinones in RCs from <i>Rhodospseudomonas</i> <i>sphaeroides</i> . By G. Feher, R.A. Isaacson, M.Y. Okamura, and W. Lubitz (With 10 Figures) .....	174
Photoinduced Charge Separation in Bacterial Reaction Centers Investigated by Triplets and Radical Pairs By J.R. Norris, D.E. Budil, S.V. Kolaczowski, J.H. Tang, and M.K. Bowman (With 5 Figures) .....	190
Spin Dipolar Interactions of Radical Pairs in Photosynthetic Reaction Centers. By A. Ogrodnik, W. Lersch, M.E. Michel-Beyerle, J. Deisenhofer, and H. Michel (With 4 Figures) .....	198
Protein/Lipid Interaction of Reaction Center and Antenna Proteins. By J. Riegler, W.M. Heckl, J. Peschke, M. Lösche, and H. Möhwald (With 6 Figures) .....	207
The Architecture of Photosystem II in Plant Photosynthesis. Which Peptide Subunits Carry the Reaction Center of PS II? By A. Trebst and B. Depka (With 3 Figures) .....	216

---

**Part III      Electron-Transfer: Theory and Model Systems**

---

Application of Electron-Transfer Theory to Several Systems of Biological Interest. By R.A. Marcus and N. Sutin .....	226
Effects of Distance, Energy and Molecular Structure on Long- Distance Electron-Transfer Between Molecules By J.R. Miller (With 4 Figures) .....	234

Ultrafast Electron Transfer in Biomimetic Models of Photosynthetic Reaction Centers. By M.R. Wasielewski, M.P. Niemczyk, W.A. Svec, and E.B. Pewitt (With 5 Figures) .....	242
Electron Transfer Through Aromatic Spacers in Bridged Electron-Donor-Acceptor Molecules. By H. Heitele and M.E. Michel-Beyerle	250
Electron Transfer in Rigidly Linked Donor-Acceptor Systems By S.F. Fischer, I. Nussbaum, and P.O.J. Scherer (With 3 Figures) .	256
Electron Conduction Along Aliphatic Chains By R. Bittl, H. Treutlein, and K. Schulten (With 4 Figures) .....	264

---

**Part IV      Reaction Centers: Structure and Dynamics**

---

Kinetics and Mechanisms of Initial Electron-Transfer Reactions in <i>Rhodospseudomonas sphaeroides</i> Reaction Centers By W.W. Parson, N.W.T. Woodbury, M. Becker, C. Kirmaier, and D. Holten (With 3 Figures) .....	278
Femtosecond Studies of the Reaction Center of <i>Rhodospseudomonas viridis</i> : The Very First Dynamics of the Electron-Transfer Processes. By W. Zinth, M.C. Nuss, M.A. Franz, W. Kaiser, and H. Michel (With 5 Figures) .....	286
Analysis of Time-resolved Fluorescence of <i>Rhodospseudomonas viridis</i> Reaction Centers By J.K.H. Hörber, W. Göbel, A. Ogorodnik, M.E. Michel-Beyerle, and E.W. Knapp (With 3 Figures) .....	292
The Characterization of the Q <sub>A</sub> Binding Site of the Reaction Center of <i>Rhodospseudomonas sphaeroides</i> . By M.R. Gunner, B.S. Braun, J.M. Bruce, and P.L. Dutton (With 2 Figures) .....	298

---

**Part V      Model Systems on Structure of Antennas  
and Reaction Centers**

---

Structure and Energetics in Reaction Centers and Semi-synthetic Chlorophyll Protein Complexes. By S.G. Boxer (With 4 Figures) ..	306
Small Oligomers of Bacteriochlorophylls as <i>in vitro</i> Models for the Primary Electron Donors and Light-Harvesting Pigments in Purple Photosynthetic Bacteria By A. Scherz, V. Rosenbach, and S. Malkin (With 7 Figures) .....	314
Experimental, Structural and Theoretical Models of Bacteriochlorophylls a, d and g. By J. Fajer, K.M. Barkigia, E. Fujita, D.A. Goff, L.K. Hanson, J.D. Head, T. Horning, K.M. Smith, and M.C. Zerner (With 6 Figures) .....	324

ENDOR Characterization of Hydrogen-Bonding to Immobilized Quinone Anion Radicals. By P.J. O'Malley, T.K. Chandrashekar, and G.T. Babcock (With 3 Figures) .....	339
Concluding Remarks. Some Aspects of Energy Transfer in Antennas and Electron Transfer in Reaction Centers of Photosynthetic Bacteria. By J. Jortner and M.E. Michel-Beyerle (With 6 Figures) .....	345
<b>Index of Contributors</b> .....	<b>367</b>

# Femtosecond Studies of the Reaction Center of *Rhodopseudomonas viridis*: The Very First Dynamics of the Electron-Transfer Processes

W. Zinth, M.C. Nuss, M.A. Franz, and W. Kaiser

Physik-Department, Technische Universität München,  
D-8000 München, F. R. G.

H. Michel

Max-Planck-Institut für Biochemie, D-8033 Martinsried, F. R. G.

The X-ray structure analysis of crystals made up of reaction centers (RC) of *Rhodopseudomonas viridis* provides us with the information on the location and orientation of the various pigments in the protein matrix /1,2/. After many years of speculation one is now in the position to predict unequivocally the path of the electron in the RC following the absorption of a photon by the special pair in the RC. This note is concerned with the time-dependence of the very first events.

We present here results from ultrafast time-resolved experiments. The RC were excited by a first ultrashort light pulse which triggered the photochemical reactions. A second, properly delayed probing pulse monitored absorbance changes induced by the various transient intermediates. The measurements with highest time resolution ( $1 \times 10^{-13}$  s) were made with exciting and probing pulses of 150 fs ( $1.5 \times 10^{-13}$  s) duration at a wavelength of 620 nm. These pulses were generated in a cw dye-laser system operating in the colliding pulse mode (CPM) /3/. The exposure of the sample to light was held on a low level by the following two techniques: First, an electro-optical modulator operating at 100 KHz cuts short pulse trains of five individual pulses from the 100 MHz repetition rate emission of the CPM laser. Second rotation of the sample cell with 25 Hz ensured that each short pulse train illuminated a new portion of RC /4/. The light intensity was kept so low that in the excited-sample volume less than  $10^{-2}$  of the reaction centers were excited. The changes of absorption were monitored by delayed probe pulses at the same wavelength. To supplement our femtosecond data, excite and probe measurements using single picosecond pulses from a Nd-glass laser system were made at different probe frequencies. Tuning of the probe pulse was achieved by frequency converters based on the stimulated Raman process. Excitation wavelength was 620 nm. In the picosecond experiments less than 15% of the RCs were excited.

The reaction centers of *Rhodopseudomonas viridis* studied here were prepared according to the procedure given in /1/. We used reaction center preparations where 20 mM ascorbate was added in order to reduce the quinones. In that way it was guaranteed that oxidized special pairs did not accumulate. The absorption spectra of the RC were studied prior to and after each experimental run. An absorbance change indicating a decomposition of

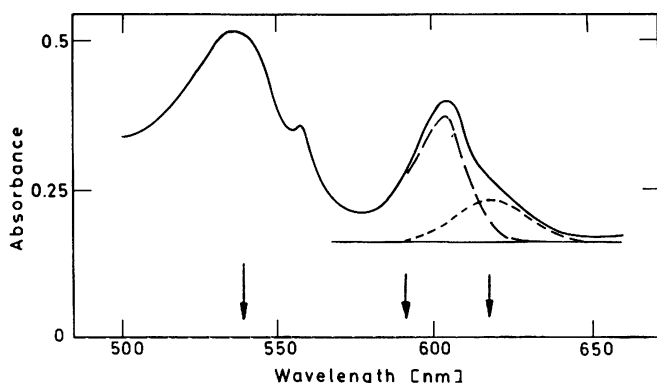


**Fig. 1** Absorbance spectrum of a suspension of reaction center preparation of *Rhodospseudomonas viridis*. The broken lines represent a decomposition of the band around 605 nm into the contributions from the  $Q_x$  transition of the accessory BChl<sub>A</sub> ( $\lambda_{\max} \sim 605$  nm) and of the special pair ( $\lambda_{\max} \sim 618$  nm). (Sample: RC without ascorbate).

the RC during the picosecond and femtosecond experiments was not observed.

In Fig.1 part of the absorption spectrum of the reaction center in solution is depicted. The band at 610 nm corresponds to the  $Q_x$  transition of the two accessory bacteriochlorophyll b molecules (BChl<sub>A</sub>) and the broad shoulder around 620 nm belongs to the  $Q_x$  transition of the special pair (P), the bacteriochlorophyll dimer. The position of the  $Q_x$  transition of P is well established from bleaching experiments /5/. Photooxidation of P reduces the absorption band at 960 nm, the  $Q_y$  transition of P, and simultaneously the absorption around 618 nm. The broad absorption at 530 nm in Fig.1 is made up of absorption bands of the two bacteriopheophytin b molecules (BPh) of the reaction center and of the four cytochrome units attached to the RC.

With light pulses of 620 nm we excited predominantly the special pair; approximately 20% of the incident radiation was absorbed by the neighboring BChl<sub>A</sub>. In Fig.2 the absorption changes, initiated by the femtosecond excitation pulse and monitored by the delayed probe pulse, are presented as a function of delay time between the two pulses. Four successive processes are readily seen in the figure: During the passage of the excitation pulse of 150 fs the absorption of the sample decreases strongly. At the end of the excitation the absorption increases very rapidly with a time constant shorter than the pulse duration. The enhanced absorption decreases for approximately 1 ps and recovers with a time constant of 5 ps.

The experimental data suggest that four transient species are seen during the first 10 ps after excitation of the special pair: A first state having reduced absorbance (at 620 nm) lives shorter than the pulse duration; a second intermediate of enhanced absorbance lasts for 1 ps, a third one lives 5 ps, and a fourth one is stable during our subsequent observation time of 100 ps.

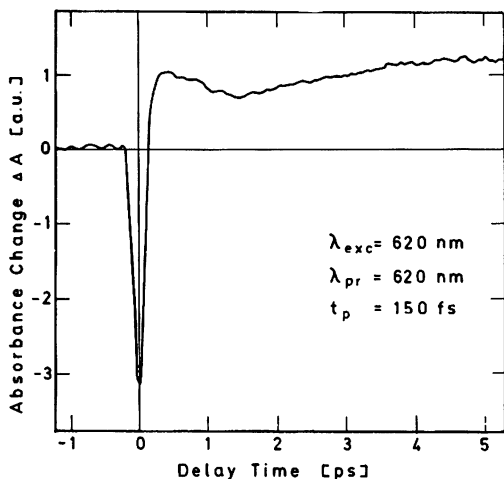


Fig. 2 Absorbance change induced by 150 fs pulses at  $\lambda = 620$  nm measured as a function of time delay at the same wavelength. The transient absorbance changes indicate the existence of four intermediate states formed after optical excitation.

The assignment of the different absorption processes of Fig. 2 to molecular states is supported by several sources of information. (i) As pointed out above, the x-ray work tells us the location of the different pigments within the protein, and thus gives strong indication on the course of the electron after excitation of the special pair. (ii) Our picosecond data (discussed below) at the frequency position of the BChl and BPh absorption bands help us to interpret our data for times exceeding 1 ps. (iii) Information on the absorption properties of the oxidized special pair  $P^+$  may be deduced from the known spectra of the state  $P^+Q^-$ . Assuming that the negative charge at the quinone does not influence the visible spectrum, we deduce that  $P^+$  has a broad absorption extending from a peak around  $1.3 \mu\text{m}$  throughout the visible. Additional spectroscopic data /6/ give information on the absorbance changes induced by reducing the pigments BChl and BPh. In Fig. 3 the absorbance changes are depicted which occur when bacteriochlorophyll b and bacteriopheophytine b are reduced chemically to form  $BChl^-$  and  $BPh^-$ , respectively. The curves in Fig. 3 (redrawn from /6/) were taken in solutions of dimethylformamide ( $BChlb^-$ ) and  $\text{CH}_2\text{Cl}_2$  ( $BPh^-$ ). While small shifts of the band are likely when going into the protein surrounding, the broad features of the spectra should basically remain unchanged, allowing the following discussion.

According to our present tentative picture the time-sequence of events is as follows: (i) During the excitation the special pair is promoted to the excited state; the reduced number of special pairs in the ground state leads to a decrease in absorption at the very beginning. The observed absorbance decrease is enhanced by the so-called coherence artifact, which exists only during the time duration of the exciting pulse. (ii) Immediately following the excitation, i.e. even during the excitation pulse of 150 fs, a second, strongly absorbing species is formed. To our

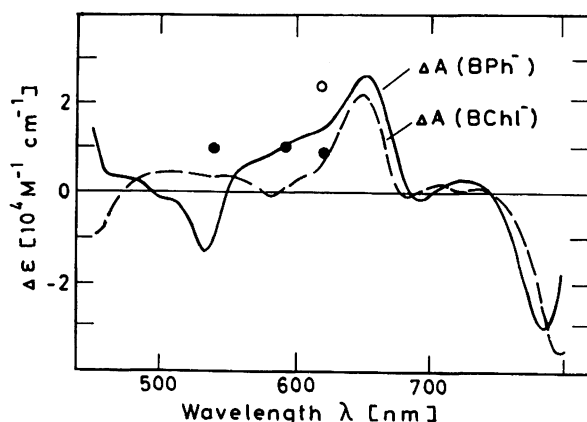


Fig. 3 Absorbance change induced by reduction of BChl<sub>b</sub> in dimethylformamide (solid curve) and of BPh<sub>b</sub> in CH<sub>2</sub>Cl<sub>2</sub> (broken curve, after /6/). Absorption changes deduced from our time-resolved data are shown for the state P<sup>+-</sup> (ΔA(P<sup>+-</sup>), open circle) and for the oxidized special pair (ΔA(P<sup>+</sup>), full circle).

interpretation, fast charge separation in the excited special pair forms the P<sup>+-</sup> state within 150 fs. (iii) The following decrease in absorption within 1 ps suggests to us the rapid passage of the electron at the neighboring BChl<sub>A</sub> forming a transient P<sup>+</sup>BChl<sub>A</sub><sup>-</sup> state. The electron continues its path to the pheophytine within 5 ps; we see a new state P<sup>+</sup>BPh<sup>-</sup>. In our samples, where the quinones are chemically reduced, back-reactions return the RC to its initial state within less than 10<sup>-4</sup> s.

Some comments should be added concerning the absolute values of the absorbance changes induced by the various intermediates. At late delay times one observes state P<sup>+</sup>BPh<sup>-</sup>. Its absorbance change ΔA is induced, in a first-order approximation, by oxidation of the special pair (giving ΔA(P<sup>+</sup>)) and reduction of a bacterio-pheophytine (ΔA(BPh<sup>-</sup>)): ΔA(P<sup>+</sup>BPh<sup>-</sup>) ≈ ΔA(P<sup>+</sup>) + ΔA(BPh<sup>-</sup>). In a similar way we obtain ΔA(P<sup>+</sup>BChl<sub>A</sub><sup>-</sup>) ≈ ΔA(P<sup>+-</sup>) + ΔA(BChl<sub>A</sub><sup>-</sup>). Knowing ΔA(BChl<sub>A</sub><sup>-</sup>) and ΔA(BPh<sup>-</sup>) from Fig.3 we can deduce from Fig.2 the values of ΔA(P<sup>+</sup>) (full circles in Fig.3) and ΔA(P<sup>+-</sup>) (open circle in Fig.3).

Additional information supporting the presented interpretation and yielding the absorbance changes ΔA(P<sup>+</sup>) at other wavelengths can be deduced from the picosecond measurements: In Fig.4 the change of absorption at 592 nm is presented after picosecond excitation at 623 nm. As pointed out in Fig.1, at 592 nm the Q<sub>x</sub> transition of BChl<sub>A</sub> absorbs stronger than the special pair. After excitation of the special pair at 623 nm the absorption at 592 nm rises during the pulse duration of 4 ps and remains constant for longer times. A more careful analysis of the data shows, however, that the build-up of the absorption is slowed down. The broken curve in the figure represents the measured integral over the autocorrelation curve. The difference between the instantaneous response and the experimental data are presented on an enlarged

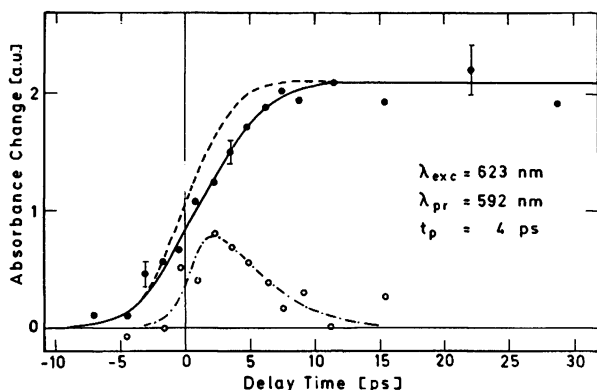


Fig. 4 Absorbance change induced by pulses at 620 nm with 4 ps duration measured at  $\lambda = 592$  nm (full circles). The broken curve shows the integrated cross-correlation curve. Differences between the solid and the broken curve are drawn in an enlarged scale ( $\times(-3)$ ) as the open circles.

scale by the dash-dotted curve. One may explain the data of Fig.4 as follows: The excitation of the special pair at 623 nm leads to an enhanced absorption at 592 nm due to the rapid generation of  $P^{+}$  and the slower formation of the final state  $P^{+}BPh^{-}$  within 5 ps. The delay in the build-up is an indication of a short-lived intermediate state, which absorbs weaker than the final state  $P^{+}BPh^{-}$ . We believe that this intermediate state is  $P^{+}BChl_A^{-}$ . Indeed, according to the data of Fig.3, the absorbance change  $\Delta A(BChl^{-})$  is considerably smaller than  $\Delta A(BPh)$  at 592 nm.

The situation at the probing frequency at 540 nm is quite different. In Fig.5 the change of absorption after picosecond excitation at 620 nm is depicted. We find a rapidly rising (within

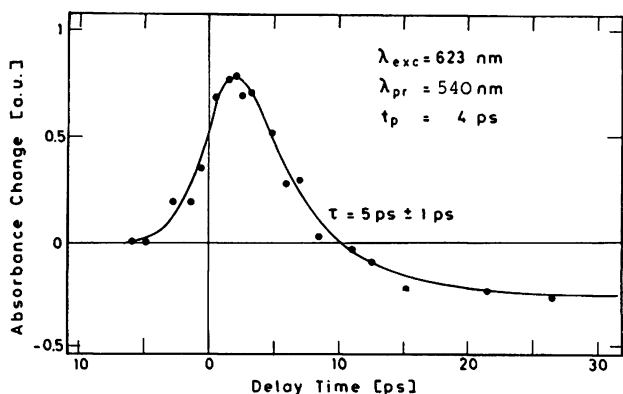
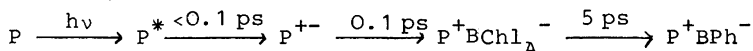


Fig. 5 Absorbance change induced by pulses at  $\lambda = 620$  nm with 4 ps duration probed at  $\lambda = 540$  nm. At this wavelength the bacterio-  
pheophytines give a negative absorbance change  $\Delta A$ . The positive  $\Delta A$  at earlier times is due to the oxidized special pair  $P^{+}$ .

the time resolution of 1 ps) enhanced absorption, followed by a negative absorption change. The short positive absorption change is believed to be due to a strong absorption of the  $P^{+-}$  and  $P^+BChl^-$  states at 540 nm. These short-lived states are not resolved with pulses of a few picosecond duration. The negative absorption change for the transition  $BPh \rightarrow BPh^-$  (see Fig.3) changes the sign of  $\Delta A$  in Fig.5. In fact, the negative values of  $\Delta A$  build up with a time-constant of 5 ps, as expected for the formation of the radical pairs  $P^+BPh^-$ . The final absorbance change is due to  $\Delta A(P^+)$  and  $\Delta A(BPh^-)$ . From a numerical fit of the measured absorbance changes we estimate  $\Delta A(P^+)$  to be 80% of  $\Delta A(BPh)$ . The value  $\Delta A(P^+)$  determined by using  $\Delta A(BPh^-)$  is shown as full circle in Fig.3. It is interesting to note that the absorbance change induced by oxidation of the special pair  $\Delta A(P^+)$  is nearly constant in the observed spectral range.

A comment should be made concerning the intramolecular energy relaxation between the  $Q_x$  state and the lower lying  $Q_y$  state of the special pair. There exists strong evidence in the literature that in large polyatomic molecules intramolecular energy relaxation in the electronic excited state proceeds very fast, within  $10^{-13}$  seconds /7/. It is very likely that the intramolecular energy relaxation in the special pair occurs during the first hundred femtoseconds prior to the formation of the  $P^{+-}$  state.

In summary we wish to say that experiments with the improved time resolution of 100 fs give new information not visible in previous picosecond experiments /8/. The proposed time sequence of charge separation and electron transfer



is consistent with the present knowledge of the reaction center and with our femtosecond and picosecond experiments.

## References

- 1 H. Michel, *J. Mol. Biol.* **158**, 567 (1982)
- 2 J. Deisenhofer, O. Epp, K. Miki, R. Huber, H. Michel, *J. Mol. Biol.* **180**, 385 (1984)
- 3 R.L. Fork, B.I. Greene, C.V. Shank, *Appl. Phys. Lett.* **38**, 671 (1981)
- 4 For details on the experimental set-up see: M.C. Nuss, W. Zinth, W. Kaiser, E. Kölling, D. Oesterhelt, *Chem. Phys. Lett.* **117**, 1 (1985)
- 5 W. Zinth, M. Sander, J. Dobler, W. Kaiser, H. Michel, same proceedings
- 6 M.S. Davis, A. Forman, T.K. Hanson, J.P. Thornber, J. Fajer, *J. Phys. Chem.* **83**, 3325 (1979)
- 7 F. Graf, A. Penzkofer, *Optics and Quant. Electron.* **17**, 53 (1985)
- 8 D. Holten, C. Hoganson, M.W. Windsor, C.C. Schenck, W.W. Parson, A. Migus, R.L. Fork, C.V. Shank, *Biochim. Biophys. Acta* **592**, 461 (1980)